NASA CR- 179,435

NASA Contractor Report 179435

Stress Concentration Around Circular Hole in a Composite Material Specimen Representative of the X-29A Forward-Swept Wing Aircraft

Hsien-Yang Yeh

Contract NGT 05020412

August 1988

National Aeronautics and
Space Administration

NASA Contractor Report 179435

Stress Concentration Around Circular Hole in a Composite Material Specimen Representative of the X-29A Forward-Swept Wing Aircraft

Hsien-Yang Yeh
Mechanical Engineering Department, California State University, Long Beach, Long Beach, California 90840

Prepared for
Ames Research Center
Dryden Flight Research Facility
Edwards, California
Under Contract NGT 05020412

1988

NASA
National Aeronautics and
Space Administration
Ames Research Center
Dryden Flight Research Facility
Edwards, California 93523-5000

CONTENTS

SUMMARY

The theory of anisotropic elasticity was used to evaluate the anisotropic stress concentration factors of a composite laminated plate containing a small circular hole. This advanced composite material was used to manufacture the X-29A forward-swept wing. Observe that the usual isotropic material stress concentration factor is three. However, for composite material, it was found that the anisotropic stress concentration factor is no longer a constant, and that the locations of maximum tangential stress points could shift by changing the fiber orientation with respect to the loading axis. The analysis showed that through the lamination process, the stress concentration factor could be reduced drastically, and therefore the structural performance could be improved. Both the mixture rule approach and the constant strain approach were used to calculate the stress concentration factor. The results predicted by the mixture rule approach were about twenty percent deviate from the experimental data. However, the results predicted by the constant strain approach matched the testing data very well. This showed the importance of the inplane shear effect on the evaluation of stress concentration factor for the X-29A composite plate.

ACKNOWLEDGEMENTS

This work was supported by the NASA-ASEE Summer Faculty Fellowship in 1987. The author is greatly indebted to Donald C. Bacon, Jr., assistant chief of research engineering division, Alan L. Carter, branch chief of aerostructures, V. Michael DeAngelis, deputy branch chief of aerostructures, Lawrence F. Reardon, group leader of structural test operation and Dr. William L. Ko, aerospace engineer for invaluable advice, experimental data collection and helpful discussions.

INTRODUCTION

The X-29A advanced technology demonstrator is sponsored by the Defense Advanced Research Projects Agency with support from NASA and the Air Force.

The X-29A features a unique forward-swept wing (Fig. 1), made of composite materials which offers weight reduction of as much as 20 percent in comparison with convention aft-swept wings.

A forward-swept wing is prone to structural divergence, because as dynamic pressure increases, forces tend to bend the leading edge up. If a divergent speed were reached, a cycle of leading edge bending, increased local angle of attack and greater wing loading could grow to cause a structural failure. The wing's high rigidity prevents divergence from occurring within the X-29A's flight envelope.

Because of their importance in aircraft design application, laminated, continuous-fiber reinforced-resin matrix composites containing through cutouts have been the subject of considerable study (refs. 1 to 5) in this paper, anisotropic plate theory was used to calculate the anisotropic stess concentration factors (SCF) for the X-29A composite plate containing a circular hole.

NOMENCLATURE

A_{ij}	equivalent modulus or extensional stiffness for a multidirectional laminate
E_1	modulus of elasticity of anisotropic plate in axis-1 direction
E_2	modulus of elasticity of anisotropic plate in axis-2 direction
$\bar{E}_1$	modulus of elasticity of laminated composite plate in axis-1 direction

$\bar{E}_2$	modulus of elasticity of laminated composite plate in axis-2 direction
$\bar{\bar{E}}_1$	transformed modulus of elasticity of single-ply in axis-1 direction
$\bar{\bar{E}}_2$	transformed modulus of elasticity of single-ply in axis-2 direction
E_α	modulus of elasticity of anisotropic plate in α direction
E_L	modulus of elasticity of single-ply to fiber direction
E_T	modulus of elasticity of single-ply transverse in fiber direction
G_{12}	shear modulus of anisotropic plate associated with $\{1,2\}$ coordinate system
$\bar{G}_{12}$	shear modulus of laminated composite plate associated with $\{1,2\}$ coordinate system
$\bar{\bar{G}}_{12}$	transformed shear modulus of single-ply in $\{1,2\}$ coordinate system
G_{LT}	shear modulus of single-ply associated with $\{L,T\}$ coordinate system
K	stress concentration factor
k	$\sqrt{\frac{E_1}{E_2}}$
N_i	stress resultant
Q_{ij}	reduced stiffness of single-ply
$\bar{Q}_{ij}$	transformed reduced stiffness of single-ply associated with $\{1,2\}$ coordinate system
ν_{12}	Poission's ratio of anisotropic plate associated with $\{1,2\}$ coordinate system
$\bar{\nu}_{12}, \bar{\nu}_{21}$	Poission's ratios of laminated composite plate associated with $\{1,2\}$ coordinate system
$\bar{\bar{\nu}}_{12}, \bar{\bar{\nu}}_{21}$	transformed Poission's ratios of single-ply in $\{1,2\}$ coordinate system
ν_{LT}	Poission's ratio of single-ply associated with $\{L,T\}$ coordinate system
ϵ_i	constant strain
σ_α	stress in α direction
σ_∞	remote tensile stress

ANALYSIS

Let axes 1,2 be the principal coordinate axes of the laminated plate, and let axes L,T be the principal material axes of the single composite ply shown in figure 2.

For an anisotropic plate containing a circular hole subjected to remote uniaxial tensile stress σ_∞, acting at an angle ϕ with respect to the principal elastic axis 1 of the plate (fig. 3), the tangential stress, σ_α and tangential stress concentration factor, $K \equiv \sigma_\alpha/\sigma_\phi$ along the circular hole boundary may be expressed as (ref. 3)

$$K \equiv \frac{\sigma_\alpha}{\sigma_\infty} = \frac{E_\alpha}{E_1}\{[-\cos^2\phi + (k+n)\sin^2\phi]k\cos^2\alpha + [(1+n)\cos^2\phi - k\sin^2\phi]\sin^2\alpha \\ - n(1+k+n)\sin\phi\cos\phi\sin\alpha\cos\alpha\} \tag{1}$$

where E_α is the modulus of elasticity in the α direction (fig. 3) given by

$$\frac{E_\alpha}{E_1} = 1 \bigg/ \left[\sin^4\alpha + \frac{E_1}{E_2}\cos^4\alpha + \frac{1}{4}\left(\frac{E_1}{G_{12}} - 2\nu_{12}\right)\sin^2 2\alpha \right] \tag{2}$$

where k and n are defined by

$$k \equiv -\mu_1\mu_2 = \sqrt{\frac{E_1}{E_2}} \tag{3}$$

$$n \equiv -i(\mu_1 + \mu_2) = \sqrt{2\left(\sqrt{\frac{E_1}{E_2}} - \nu_{12}\right) + \frac{E_1}{G_{12}}} \tag{4}$$

where $i \equiv \sqrt{-1}$, and μ_1 and μ_2 are the complex roots of the anisotropic plate characteristic equation

$$\mu^4 + \left(\frac{E_1}{G_{12}} - 2\nu_{12}\right)\mu^2 + \frac{E_1}{E_2} = 0 \tag{5}$$

For isotropic materials $k = 1$ and $n = 2$, and the stress concentration factor K (eq. (1)) reduces to

$$K = \frac{\sigma_\alpha}{\sigma_\infty} = 1 - 2\cos 2(\alpha - \phi) \tag{6}$$

which gives $K = -1$ at $(\alpha - \phi) = 0$ or π, and $K = 3$ at $(\alpha - \phi) = \pm\pi/2$.

To evaluate the modulus of elasticity of a laminated plate, both the mixture rule approach and the constant strain approach could be used. In the mixture rule approach, the transformed ply-elastic constants $\{\bar{\bar{E}}_1, \bar{\bar{E}}_2, \bar{\bar{G}}_{12}, \bar{\bar{\nu}}_{12}, \bar{\bar{\nu}}_{21}\}$ with respect to the $\{1, 2\}$ system can be related to the material constants $\{E_L, E_T, G_{LT}, \nu_{LT}, \nu_{TL}\}$ with respect to the $\{L, T\}$ system through the following equations (refs. 6 and 7).

$$\begin{aligned}
\bar{\bar{E}}_1 &= E_L \bigg/ \left[\cos^4\Theta + \frac{E_L}{E_T}\sin^4\Theta + \frac{1}{4}\left(\frac{E_L}{G_{LT}} - 2\nu_{LT}\right)\sin^2 2\Theta \right] \\
\bar{\bar{E}}_2 &= E_L \bigg/ \left[\sin^4\Theta + \frac{E_L}{E_T}\cos^4\Theta + \frac{1}{4}\left(\frac{E_L}{G_{LT}} - 2\nu_{LT}\right)\sin^2 2\Theta \right] \\
\bar{\bar{G}}_{12} &= E_L \bigg/ \left[1 + 2\nu_{LT} + \frac{E_L}{E_T} - \left(1 + 2\nu_{LT} + \frac{E_L}{E_T} - \frac{E_L}{G_{LT}}\right)\cos^2 2\Theta \right] \\
\bar{\bar{\nu}}_{12} &= \frac{E_1}{E_L}\left[\nu_{LT} - \frac{1}{4}\left(1 + 2\nu_{LT} + \frac{E_L}{E_T} - \frac{E_L}{G_{LT}}\right)\sin^2 2\Theta \right] \\
\bar{\bar{\nu}}_{21} &= \frac{E_2}{E_L}\left[\nu_{LT} - \frac{1}{4}\left(1 + 2\nu_{LT} + \frac{E_L}{E_T} - \frac{E_L}{G_{LT}}\right)\sin^2 2\Theta \right]
\end{aligned} \tag{7}$$

If the composite plate is made of N number of single plies with different fiber orientations, then by using the mixture rule, the engineering elastic constants $\{\bar{E}_1, \bar{E}_2, \bar{G}_{12}, \bar{\nu}_{12}, \bar{\nu}_{21}\}$ for the composite plate can be written as

$$\bar{E}_1 = \frac{1}{N}\sum_{j=1}^{N} \bar{\bar{E}}_1(\Theta_j)$$

$$
\begin{aligned}
\bar{E}_2 &= \frac{1}{N}\sum_{j=1}^{N}\bar{\bar{E}}_2(\Theta_j)\\
\bar{G}_{12} &= \frac{1}{N}\sum_{j=1}^{N}\bar{\bar{G}}_{12}(\Theta_j)\\
\bar{\nu}_{12} &= \frac{1}{N}\sum_{j=1}^{N}\bar{\bar{\nu}}_{12}(\Theta_j)\\
\bar{\nu}_{21} &= \frac{1}{N}\sum_{j=1}^{N}\bar{\bar{\nu}}_{21}(\Theta_j)
\end{aligned}
\tag{8}
$$

In the constant strain approach, it is assumed that the strain remains constant across the laminate thickness and the inplane stress-strain relation for a laminate is used and it is actually the stress resultant versus inplane strain relation.

$$
\begin{aligned}
N_1 &= A_{11}\epsilon_1 + A_{12}\epsilon_2 + A_{16}\epsilon_6\\
N_2 &= A_{21}\epsilon_1 + A_{22}\epsilon_2 + A_{26}\epsilon_6\\
N_6 &= A_{61}\epsilon_1 + A_{62}\epsilon_2 + A_{66}\epsilon_6
\end{aligned}
\tag{9}
$$

where A_{ij} are defined by (refs. 6 and 7)

$$
A_{ij} = \sum_{k=1}^{N}(\bar{Q}_{ij})_k(z_k - z_{k-1}) \qquad i,j = 1,2,6 \tag{10}
$$

in which

$$
\begin{aligned}
\bar{Q}_{11} &= Q_{11}\cos^4\theta + 2(Q_{12} + 2Q_{66})\sin^2\theta\cos^2\theta + Q_{22}\sin^4\theta\\
\bar{Q}_{12} &= (Q_{11} + Q_{22} - 4Q_{66})\sin^2\theta\cos^2\theta + Q_{12}(\sin^4\theta + \cos^4\theta)\\
\bar{Q}_{22} &= Q_{11}\sin^4\theta + 2(Q_{12} + 2Q_{66})\sin^2\theta\cos^2\theta + Q_{22}\cos^4\theta\\
\bar{Q}_{16} &= (Q_{11} - Q_{12} - 2Q_{66})\sin\theta\cos^3\theta + (Q_{12} - Q_{22} + 2Q_{66})\sin^3\theta\cos\theta\\
\bar{Q}_{26} &= (Q_{11} - Q_{12} - 2Q_{66})\sin^3\theta\cos\theta + (Q_{12} - Q_{22} + 2Q_{66})\sin\theta\cos^3\theta\\
\bar{Q}_{66} &= (Q_{11} + Q_{22} - 2Q_{12} - 2Q_{66})\sin^2\theta\cos^2\theta + Q_{66}(\sin^4\theta + \cos^4\theta)
\end{aligned}
\tag{11}
$$

and

$$
\begin{aligned}
Q_{11} &= \frac{E_L}{1 - \nu_{LT}\nu_{TL}}\\
Q_{12} &= \frac{\nu_{LT}E_T}{1 - \nu_{LT}\nu_{TL}} = \frac{\nu_{TL}E_L}{1 - \nu_{LT}\nu_{TL}}\\
Q_{22} &= \frac{E_T}{1 - \nu_{LT}\nu_{TL}}\\
Q_{66} &= G_{LT}
\end{aligned}
\tag{12}
$$

The calculation of the effective engineering elastic constants $\{\bar{E}_1, \bar{E}_2, \bar{G}_{12}, \bar{\nu}_{12}\}$ is performed by relating the compliance components to inplane engineering constants under uniaxial tension along the 1-axis (ref. 8).

RESULTS

The X-29A forward-swept wing composite plate is made up of 40-plies with the total thickness of .56 cm (.22 in). The stacking sequence and the ply-engineering elastic constants are given by

$$[\pm 45 | 0_4 | \pm 45 | 90_2 | \pm 45 | 0_4 | \pm 45 | 0_2]_s$$

$$E_L = 18.76 \times 10^6 psi$$
$$E_T = 1.57 \times 10^6 psi$$
$$G_{LT} = 0.82 \times 10^6 psi$$
$$\nu_{LT} = 0.312$$

By replacing $\{E_1, E_2, G_{12}, \nu_{12}\}$, respectively, with $\{\bar{E}_1, \bar{E}_2, \bar{G}_{12}, \bar{\nu}_{12}\}$ in equations (1), (2), (3), and (4), the tangential stresses σ_α around a circular hole in a laminated X-29A composite plate were calculated for three loading cases: $\phi = 0$ (loading in axis-1 direction), $\phi = \frac{\pi}{4}$, and $\phi = \frac{\pi}{2}$ (loading in axis-2 direction). The results obtained from the constant strain approach and the mixture rule approach are ploted in figures 4 to 6 and figures 7 to 9 respectively. Figure 4 shows the plot of σ_α for the laminated X-29A composite material when the plate is under uniaxial tension in the composite elastic axis-1 direction. The maximum stress concentration factor K for the laminated X-29A composite plate reached the peak value of 3.614 (larger than 3) at two locations ($\alpha = 90°$ and $\alpha = 270°$). When the loading axis is $\phi = \frac{\pi}{4}$ oblique to the composite axis-1 (fig. 5), the maximum stress concentration factor K reaches the value of 3.033 at two locations ($\alpha = 120°$ and $\alpha = 300°$). When the loading axis is parallel to the composite elastic axis-2 (fig. 6), the maximum stress concentration factor K drops to the value of 2.708 at two locations ($\alpha = 0°$ and $\alpha = 180°$).

Again, figure 7 shows the plot of σ_α for the laminated X-29A composite material when the plate is under uniaxial tension in the composite elastic axis-1 direction. The maximum stress concentration factor K for the laminated X-29A composite plate reached the peak value of 4.475 (higher than 3.614 in figure 4) at two locations ($\alpha = 90°$ and $\alpha = 270°$). When the loading axis is $\phi = \frac{\pi}{4}$ oblique to the composite axis-1 (fig. 8), the maximum stress concentration factor K drops to the value of 2.977 (lower than 3.033 in figure 5) at two locations ($\alpha = 100°$ and $\alpha = 290°$). When the loading axis is parallel to the composite elastic axis-2 (fig. 9), the maximum stess concentration factor K reaches the value of 3.021 (higher than 2.708 in figure 6) at two locations ($\alpha = 0°$ and $180°$). Finally, figures 4 to 6 and figures 7 to 9 are summarized in Table 1 and Table 2, respectively.

For comparison purposes, similar calculations were made for a single-ply of the X-29A composite using equation (1). When loading is along the fiber direction (axis L, fig. 10), the maximum stress concentration factor K reaches the peak value of 6.401 at two locations ($\alpha = 90°$ and $\alpha = 270°$). When the loading is $\frac{\pi}{4}$ oblique to the fiber direction (fig. 11), the maximum K value is 3.988 at two locations ($\alpha = 100°$ and $\alpha = 280°$). When the loading direction is transverse to the fiber direction (axis T, fig. 12), the maximum value of K is -3.457 at two points ($\alpha = 90°$ and $\alpha = 270°$). The negative sign of K value represents a compressive stress concentration. Table 3 is used to summarize the results from figures 10 to 12. For reference purposes, the stress concentration factor of isotropic material is plotted in figures 13 and 14.

The stress concentration factors evaluated from different approaches (mixture rule and constant strain) discussed previously were compared by performing simple coupon tests. The width W of the rectangular specimen is 3.81 cm (1.5 in) and the diameter of the small central circular hole is .635 cm (0.25 in). The comparison of stress concentration factors between theoretical predictions and experimental results are listed in table 4. The comparison of stress concentration factors between single-ply and laminated plate are shown in table 5.

A simple FORTRAN program for calculating anisotropic stress concentration factors is listed in the appendix.

CONCLUSION

The theory of anisotropic elasticity was used to evaluate the anisotropic stress concentration factors for single-ply and laminated OBX-29A (forward-swept wing) research aircraft composite plates, each of which contained a small circular hole.

It is well known that the usual isotropic material stress concentration factor is three. However, the analysis showed that the anisotropic stress concentration factor could be greater or less than three for composite materials, and the locations of the maximum tangential stress points could shift by the change of fiber orientation with respect to the loading axis.

It was found that through the lamination process the stress concentration factor could be reduced drastically, and therefore the structural performance could be improved. The next logical step in the study of anisotropic stress concentration problem would be to know the optimum lamination process to obtaining the minimum stress concentration factors of laminate plates. This is a subject that may need further studies.

Both the mixture rule approach and the constant strain approach were used to calculate stress concentration factors. The results obtained by the mixture rule approach were about twenty percent deviate from the experimental data. However, the results predicted by the constant strain approach matched the testing data very well. This showed the importance of the inplane shear effect on the evaluation of stress concentration factors for the laminated X-29A composite plate. A further investigation about the inplane shear effect will need a three dimensional model from anisotropic elasticity plus the interlaminar stress analysis.

The anisotropic stress concentration of laminated plates is a difficult and complicated problem. To obtain a better understanding of this physical phenomenon, consideration of the hole size effect and utilization, the theory of linear elastic fracture mechanics, and the theory of micromechanics is imperative.

REFERENCES

1. Ko, W.L.: *Stress Concentration Around a Small Circular Hole in the HiMAT Composite Plate*, NASA TM-86038, Dec. 1985.

2. Savin, G.N.: *Stress Distribution Around Holes*, NASA TT F-607, 1970.

3. Lekhnitskii, S.G.; Tsai, S.W.; and Cheron, T.: *Anisotropic Plates*. Gordon and Breach Science Publishers, New York, 1968.

4. Nuismer, R.J.; and Whitney, J.M.: Uniaxial failure of composite laminates containing stress concentrations. In *Fracture Mechanics of Composites*, ASTM ATP 593, 1975, pp. 117–142.

5. Whitney, J.M.: and Nuismer, R.J.: Stress fracture criteria for laminated composite containing stress concentration. *J. Comp. Materials*, vol. 8, pp. 253–265, 1974.

6. Calote, L.R.: *The Analysis of Laminated Composite Structures*. Van Nostrand Reinhold Co., New York, 1969.

7. Jones, R.M.: *The Mechanics of Composite Materials*. McGraw-Hill Book Co., New York, 1975.

8. Tsai, S.W.; and Hahn, H.T.: *Introduction to Composite Materials*. Technomic Publishing Company, Inc., 1980.

TABLE 1. Stress Concentration Factors for an X-29A Laminated Plate 40-Plies $[\pm 45 | 0_4 | \pm 45 | 90_2 | \pm 45 | 0_4 | \pm 45 | 0_2]_s$ Constant Strain Approach

ϕ	0°	45°	90°
K	3.614	3.033	2.708
α	90°, 270°	120°, 300°	0°, 180°

ϕ: orientation of loading axis
K: stress concentration factor
α: locations of peak stress

TABLE 2. Stress Concentration Factors for an X-29A Laminated Plate 40-Plies $[\pm 45 | 0_4 | \pm 45 | 90_2 | \pm 45 | 0_4 | \pm 45 | 0_2]_s$ Mixture Rule Approach

ϕ	0°	45°	90°
K	4.475	2.977	3.021
α	90°, 270°	110°, 290°	0°, 180°

ϕ: orientation of loading axis
K: stress concentration factor
α: locations of peak stress

Table 3. Stress Concentration Factors for a Single-Ply of X-29A Composite

ϕ	0°	45°	90°
K	6.401	3.988	-3.457
α	90°, 270°	100°, 280°	90°, 270°

ϕ: orientation of loading axis
K: stress concentration factor
α: locations of peak stress

TABLE 4. Comparison of Stress Concentration Factors

Loading (lb)	Constant strain	Mixture rule	Experimental results
600	3.614	4.475	3.627
1000	3.614	4.475	3.506
2000	3.614	4.475	3.567
3000	3.614	4.475	3.546
4000	3.614	4.475	3.506

$\phi = 0°$: orientation of loading axis
$\alpha = 90°, 270°$: locations of peak stress

TABLE 5. Comparison of Stress Concentration Factors

Single ply	Laminated plate	
	Constant strain	Mixture rule
6.401	3.614	4.475

$\phi = 0°$: orientation of loading axis
$\alpha = 90°, 270°$: locations of peak stress

APPENDIX

```
C NSCF.FOR NASA X29 WING STRESS CONCENTRATION FACTOR
      WRITE (*,10)
   10 FORMAT ('INPUT E1,E2,V12,G12',/)
      READ (*,20) E1,E2,V12,G12
   20 FORMAT ( 4E12.5)
      WRITE (*,21)
   21 FORMAT (2X,'E1', 4X,'E2',4X,'V12',4X,'G12')
      WRITE (*, 22) E1,E2,V12,G12
   22 FORMAT (4E12.5)
      EOE=E1/E2
      EOG=E1/G12
      SK=(EOE)**.5
      SN=(2*(SK-V12)+EOG)**.5
      PI=3.14159265359
      PHI=0.
      DO 100 L=1,3
      RPHI=PHI*PI/180.
      SSI=SIN(RPHI)
      CCO=COS(RPHI)
      IF ( ABS(SSI).LE. .0000001) GO TO 101
      IF ( ABS(CCO).LE. .0000001) GO TO 102
      GO TO 110
  101 SSI=0.
      GO TO 110
  102 CCO=0.
      GO TO 110
  110 CC2=CCO*CCO
      SS2=SSI*SSI
      CCSS=CCO*SSI
      AN=0.
      DO 30 K=1,73
      ALFA=AN*PI/180.
      SI=SIN(ALFA)
      CO=COS(ALFA)
      IF ( ABS (SI). LE. .0000001) GO TO 31
      IF ( ABS (CO). LE. .0000001) GO TO 32
      GO TO 40
   31 SI=0.
      GO TO 40
   32 CO=0.
      GO TO 40
   40 CS=SI*CO
      C2=CO*CO
      S2=SI*SI
      C4=C2*C2
      S4=S2*S2
      EAFA=E1/(S4+EOE*C4+(EOG-2*V12)*S2*C2)
      AA=(-CC2+(SK+SN)*SS2)*SK*C2
      BB=((1+SN)*CC2-SK*SS2)*S2
      DD=-SN*(1+SK+SN)*CS*CCSS
      SCF=(EAFA/E1)*(AA+BB+DD)
      WRITE (*,200)
      WRITE (*,210)PHI, AN, SCF
      AN=AN+5.
      WRITE (*,300)
```

```
300   FORMAT (2X,'ANGLE ALPHA =AN =LOCATION OF STRESS POINT')
      WRITE (*, 310) AN
310   FORMAT (E12.4)
 30   CONTINUE
      WRITE (*,350)
350   FORMAT (2X,'ANGLE PHI= LOADING AXIS')
      WRITE (*, 360) PHI
360   FORMAT (2X,E12.4)
      PHI=PHI+45.
100   CONTINUE
      WRITE (*,200)
200   FORMAT (2X,'PHI' 8X,'AN', 8X, 'SCF')
      WRITE (*,210) PHI, AN, SCF
210   FORMAT (3E14.4)
      STOP
      END
```

```
C XAIJ.FOR NASA X29 WING IN-PLANE STIFFNESS
      WRITE (*,10)
 10   FORMAT('INPUT INT-L, E1, E2, V12, G12',/)
      READ (*,20) L, E1, E2, V12, G12
      DIMENSION Z(24), TK1(23)
 20   FORMAT (2X, I4,4E12.5)
      DATA ( TK1(I),I=1,23) / 45.,-45.,0.,45.,-45.,90.,45.,-45.,0.,
     A 45.,-45.,0.,-45.,45.,0.,-45.,45.,90.,-45.,45.,0.,-45.,45./
      DATA (Z(I),I=1,24) / -.11,-.1045,-.099,-.077,-.0715,-.066,
     A -.055,-.0495,-.044,-.022,-.0165,-.011,.011,.0165,.022,.044,
     A .0495,.055,.066,.0715,.077,.099,.1045,.11/
      PI=3.14159265359
        V21=E2*V12/E1
        DUM=1.-V12*V21
        R11=E1/DUM
        R12=V12*E2/DUM
        R22=E2/DUM
        R66=G12
        A11=0.
        A12=0.
        A16=0.
        A22=0.
        A26=0.
        A66=0.
        DO 30 K=1,L
        TK=PI*TK1(K)/180.
        SI=SIN(TK)
        CO=COS(TK)
        IF (ABS(SI) .LE. .0000001) GO TO 9
        IF (ABS(CO) .LE. .0000001) GO TO 19
        GO TO 29
  9     SI=0.
        GO TO 29
 19     CO=0.
 29     CD=SI*CO
        C2=CO*CO
        D2=SI*SI
        C4=C2*C2
        D4=D2*D2
        Q11=R11*C4+2.*(R12+2.*R66)*C2*D2+R22*D4
        Q12=(R11+R22-4.*R66)*D2*C2+R12*(D4+C4)
        Q22=R11*D4+2.*(R12+2.*R66)*D2*C2+R22*C4
        Q16=(R11-R12-2.*R66)*C2*CD+(R12-R22+2.*R66)*D2*CD
        Q26=(R11-R12-2.*R66)*CD*D2+(R12-R22+2.*R66)*CD*C2
        Q66=(R11+R22-2.*R12-2.*R66)*C2*D2+R66*(D4+C4)
        ZD=Z(K+1)-Z(K)
        A11=A11+Q11*ZD
        A12=A12+Q12*ZD
        A22=A22+Q22*ZD
        A16=A16+Q16*ZD
        A26=A26+Q26*ZD
        A66=A66+Q66*ZD
 30     CONTINUE
        WRITE (*, 100)
 100    FORMAT (4X,'A11',4X,'A12',4X,'A16',4X,'A22',4X,'A26',
```

```
     A   4X,'A66')
         WRITE (*,110) A11,A12,A16,A22,A26,A66
  110    FORMAT (6E12.4)
         STOP
         END
```

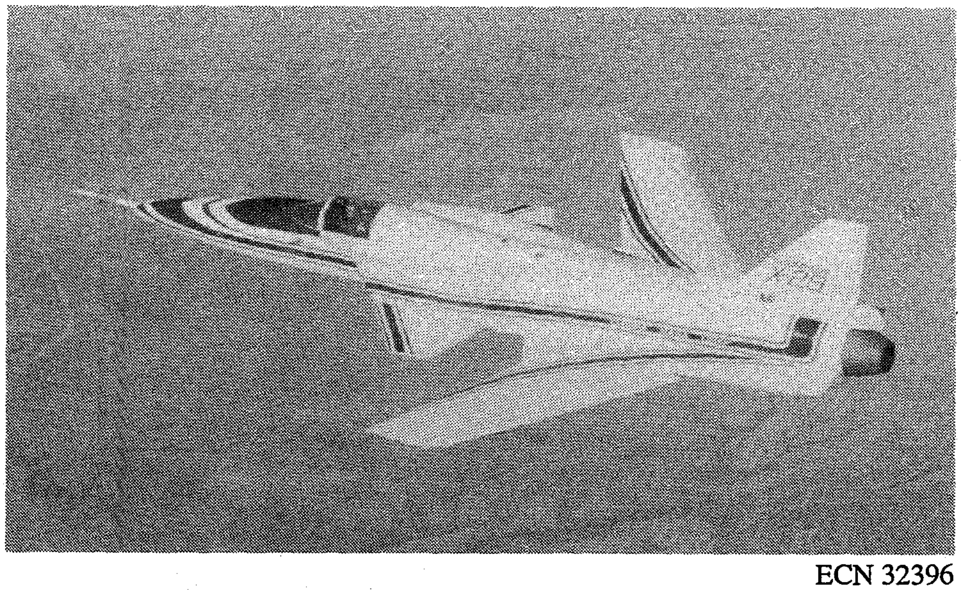

Figure 1. X-29A airplane.

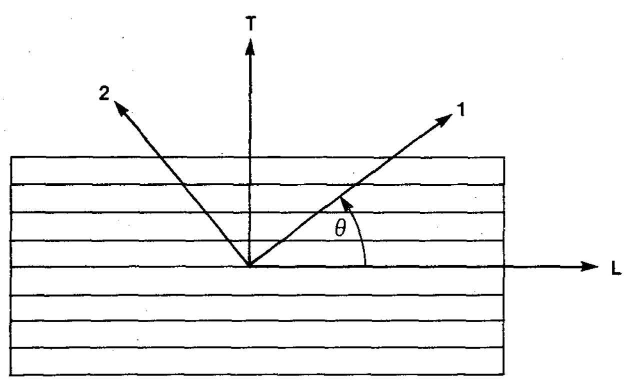

Figure 2. Rotation from material axis L to laminated plate axis 1.

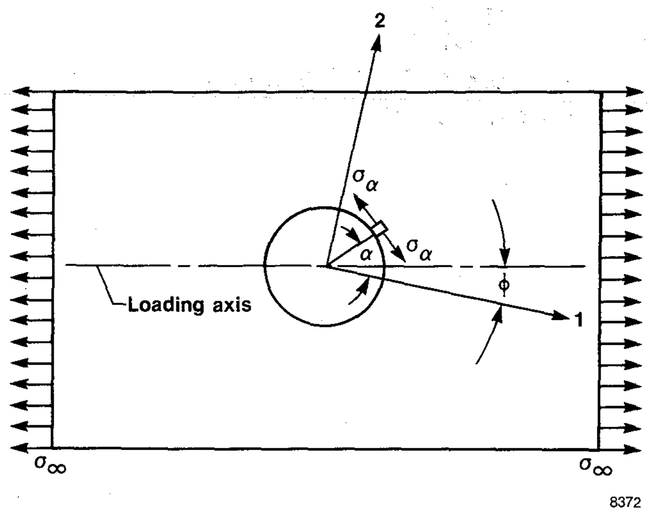

Figure 3. Tension at an angle to a principal elastic axis 1 of an anisotropic plate with a circular hole.

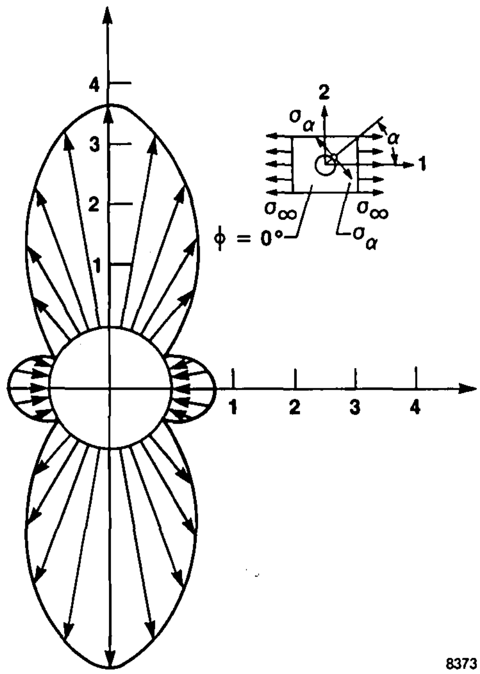

Figure 4. SCF of X-29 laminated plate (constant strain).

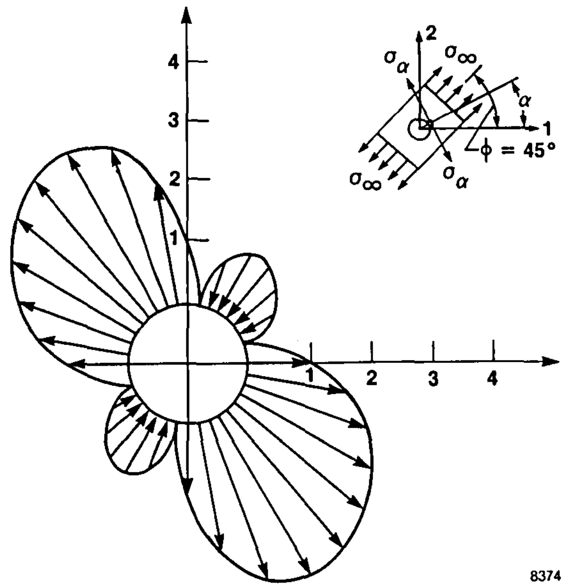

Figure 5. SCF of X-29 laminated plate (constant strain).

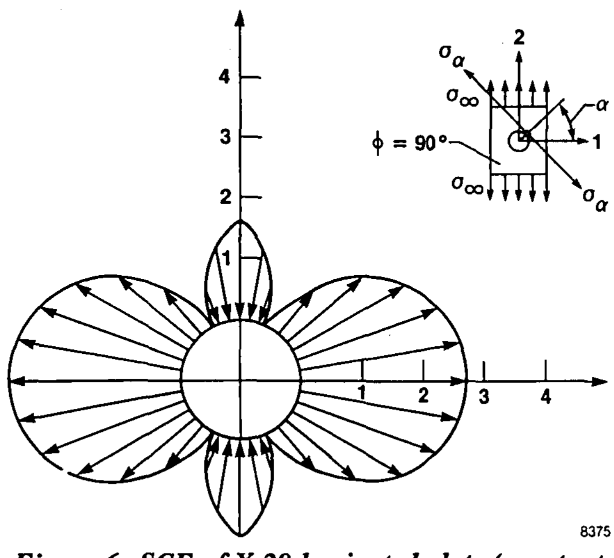

Figure 6. SCF of X-29 laminated plate (constant strain).

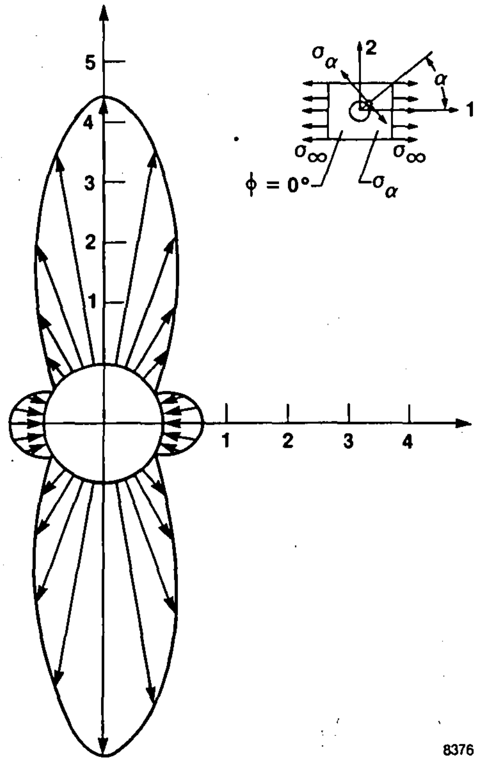

Figure 7. SCF of X-29 laminated plate (mixture rule).

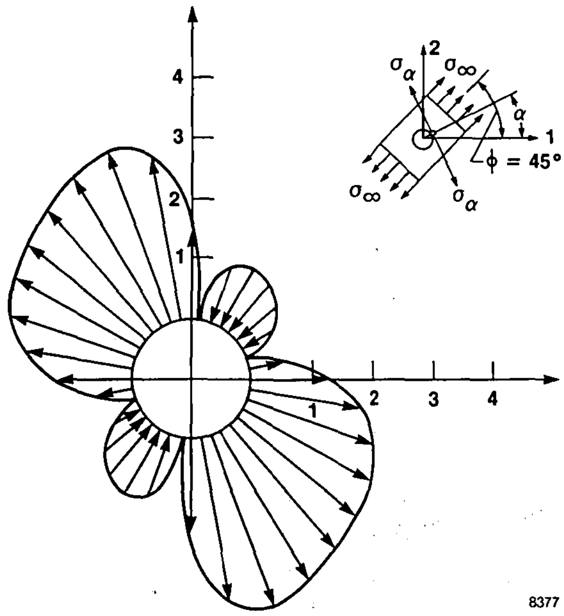

Figure 8. SCF of X-29 laminated plate (mixture rule).

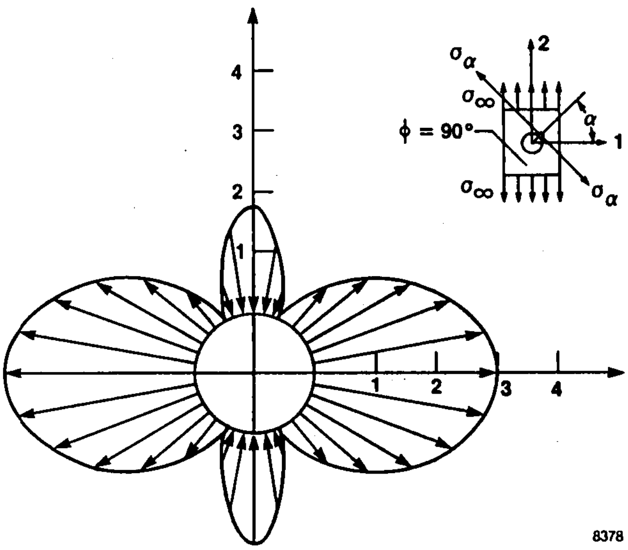

Figure 9. SCF of X-29 laminated plate (mixture rule).

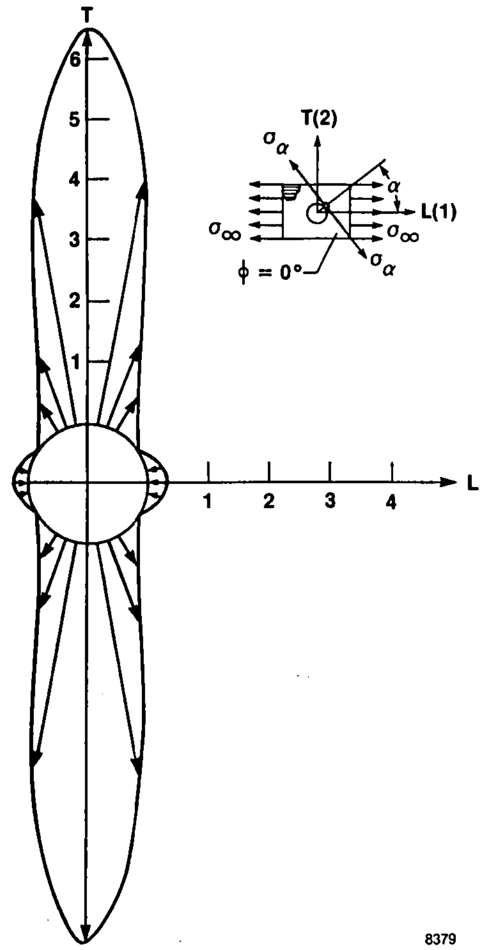

Figure 10. SCF of X-29 single ply ($\phi = 0$).

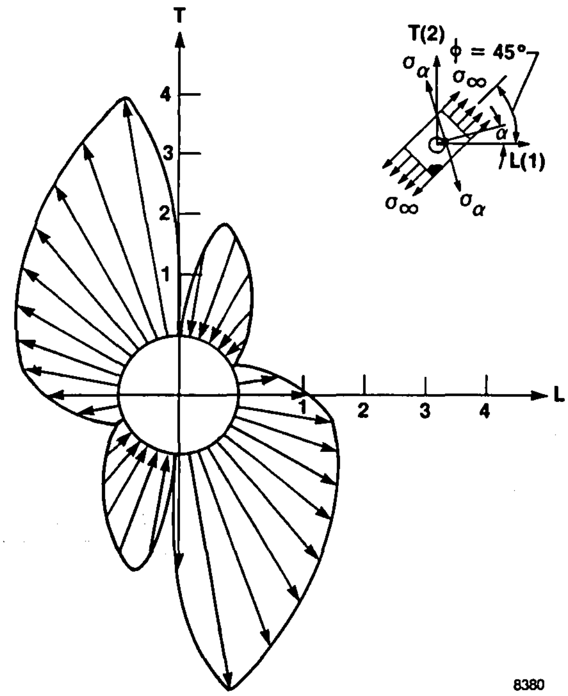

Figure 11. SCF of X-29 single ply ($\phi = \pi/4$).

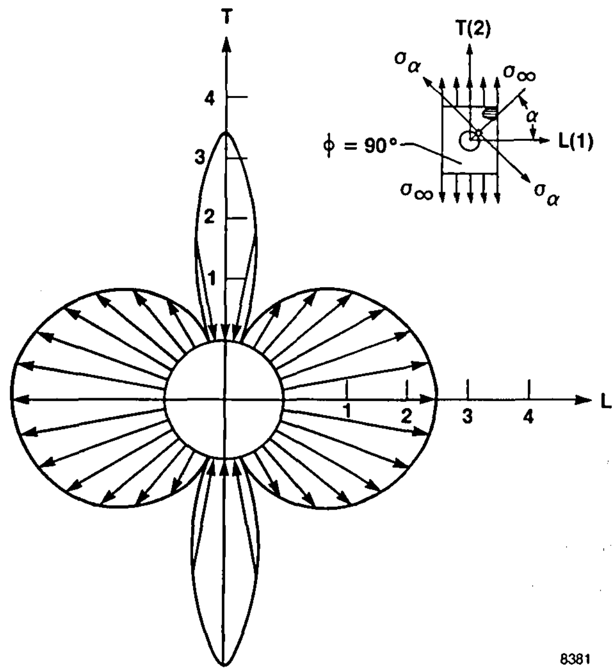

Figure 12. SCF of X-29 single ply ($\phi = \pi/2$).

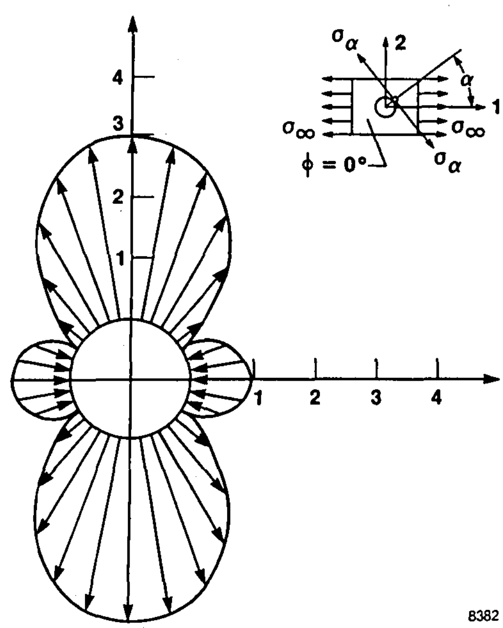

Figure 13. SCF of an isotropic plate.

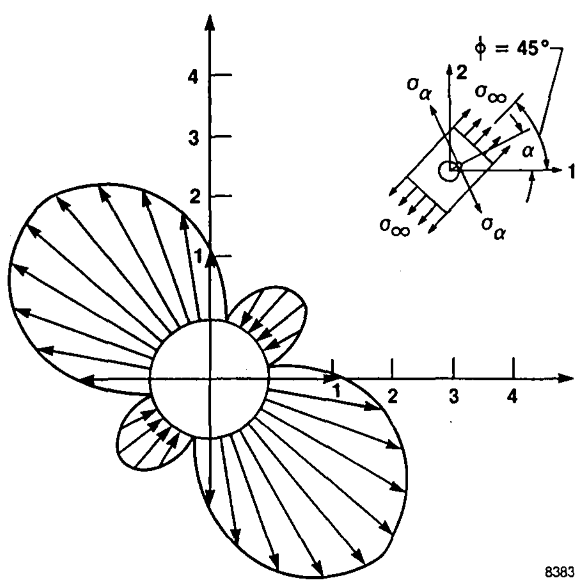

Figure 14. SCF of an isotropic plate.

NASA
National Aeronautics and Space Administration

Report Documentation Page

1. Report No. NASA CR-179435	2. Government Accession No.	3. Recipient's Catalog No.

4. Title and Subtitle

Stress Concentration Around Circular Hole in a Composite Material Specimen Representative of the X-29A Forward-Swept Wing Aircraft

5. Report Date: August 1988

6. Performing Organization Code

7. Author(s)

Hsien-Yang Yeh

8. Performing Organization Report No.: H-1435

10. Work Unit No.: RTOP 533-02-51

9. Performing Organization Name and Address

Mechanical Engineering Dept.
California State University, Long Beach
1250 Bellflower Blvd., Long Beach, California

11. Contract or Grant No.: NGT 05020412

12. Sponsoring Agency Name and Address

National Aeronautics and Space Administration
Washington, DC 20546

13. Type of Report and Period Covered: Contractor Report-Final

14. Sponsoring Agency Code

15. Supplementary Notes

NASA Technical Monitor: V. Michael Deangelis, Ames Research Center, Dryden Flight Research Facility, Edwards, California 93523-5000

16. Abstract

The theory of anisotropic elasticity was used to evaluate the anisotropic stress concentration factors of a composite laminated plate containing a small circular hole. This advanced composite material was used to manufacture the X-29A forward-swept wing. Observe that the usual isotropic material stress concentration factor is three. However, for composite material, it was found that the anisotropic stress concentration factor is no longer a constant, and that the locations of maximum tangential stress points could shift by changing the fiber orientation with respect to the loading axis. The analysis showed that through the lamination process, the stress concentration factor could be reduced drastically, and therefore the structural performance could be improved. Both the mixture rule approach and the constant strain approach were used to calculate the stress concentration factor. The results predicted by the mixture rule approach were about twenty percent deviate from the experimental data. However, the results predicted by the constant strain approach matched the testing data very well. This showed the importance of the inplane shear effect on the evaluation of stress concentration factor for the X-29A composite plate.

17. Key Words (Suggested by Author(s))	18. Distribution Statement
Composite plate Stress Concentration Circular Hole	Unclassified — Unlimited Subject category 39

19. Security Classif. (of this report)	20. Security Classif. (of this page)	21. No. of pages	22. Price
Unclassified	Unclassified	20	A02

NASA FORM 1626 OCT 86

**For sale by the National Technical Information Service, Springfield, VA 22161-2171.*

End of Document